ORIGINAL ARTICLE

Tumor immune microenvironment in cancer patients with leukocytosis

Kyung Hwan Kim[1,2] · Nam Suk Sim[1] · Jee Suk Chang[2] · Yong Bae Kim[2]

Abstract

Tumor-related leukocytosis (TRL) is correlated with poor survival in various types of cancers, but the microenvironment of TRL-associated human tumors has not been fully elucidated. Here, we aimed to characterize the immune microenvironment of cancer patients with TRL. The transcriptional signatures of tumor tissues obtained from cervical cancer patients with (TRL^{pos}) and without TRL (TRL^{neg}) were compared. As a surrogate for TRL diagnosis, a leukocytosis signature (LS) score was derived using genes differentially expressed between TRL^{pos} and TRL^{neg} tumors. The immunological profiles of patients in the TCGA database with high (LS^{high}) or low LS scores were compared. TRL^{pos} tumors were transcriptionally distinct from TRL^{neg} tumors, exhibiting up-regulation of radioresistance and down-regulation of adaptive immune response-related genes. In the TCGA cervical cancer cohort ($n = 303$), patients with high LS had inferior survival rates compared to those with low LS ($P = 0.023$). LS^{high} tumors were enriched in radioresistance, wound healing, and myeloid-derived suppressor cell (MDSC) signatures and had a higher infiltration of M2 macrophages and a lower infiltration of M1 macrophages and lymphocytes. LS^{high} tumors also expressed higher levels of CXCR2 chemokines, *CSF2*, and *CSF3*. In the pan-cancer cohort ($n = 9984$), LS^{high} tumors also exhibited poor survival, signatures of a suppressive immune microenvironment, and higher expression of CXCR2 chemokines. Our data provide evidence for a suppressive immune microenvironment in patients with TRL and suggest promising targets, such as the CXCR2 axis, for its therapeutic intervention.

Keywords Leukocytosis · Tumor microenvironment · Tumor immune evasion · Gene signatures · CXCR2

Abbreviations

BCR	B cell receptor
DEG	Differentially expressed gene
FFPE	Formalin-fixed paraffin-embedded
G-CSF	Granulocyte colony-stimulating factor
GSEA	Gene set enrichment analysis
GM-CSF	Granulocyte–macrophage colony-stimulating factor
GO	Gene ontology
GSVA	Gene set variation analysis
IFN	Interferon
LS	Leukocytosis signature
M-CSF	Macrophage colony-stimulating factor
MDSC	Myeloid-derived suppressor cells
NLR	Neutrophil-to-lymphocyte ratio
PD-1	Programmed death-1
TAM	Tumor-associated macrophage
TCGA	The cancer genome atlas
TCR	T cell receptor
TGF	Transforming growth factor
TRL	Tumor-related leukocytosis

✉ Yong Bae Kim
  ybkim3@yuhs.ac

1 Graduate School of Medical Science and Engineering, Korea Advanced Institute of Science and Technology, Daejeon, Republic of Korea

2 Department of Radiation Oncology, Yonsei Cancer Center, Yonsei University College of Medicine, Seoul, Republic of Korea

Introduction

Growing evidence suggests that there is a link between cancer and inflammation [1]. Inflammatory response is considered as one of the hallmarks of cancer and plays central roles at different stages of tumor development and progression [2, 3]. Cancer-related inflammation is known to

have tumor-promoting effects by aiding survival of cancer cells, promoting angiogenesis, and suppressing anti-tumor immunity [1]. In 10–20% cancer patients, such inflammatory responses are reflected in peripheral blood as increases in leukocytes referred to as tumor-related leukocytosis (TRL). TRL is associated with a poor response to radiotherapy or chemotherapy and, accordingly, poor survival [4–7]. Despite the dismal prognosis of patients with TRL, there is no effective therapy for such patients.

Myeloid cells, such as myeloid-derived suppressor cells (MDSCs) and tumor-associated macrophages (TAMs), are key components of tumor microenvironment inflammatory responses [8, 9]. MDSCs and TAMs aid tumor development by promoting the cellular stemness of cancer cells, angiogenesis, and epithelial–mesenchymal transition and inhibiting anti-tumor T cell responses [10]. Preclinical studies have shown that increased G-CSF secretion from tumor cells can increase both circulating and intra-tumoral MDSCs [4, 11]. In humans, TRL is associated with a higher frequency of circulating MDSCs and higher G-CSF concentrations [4, 11, 12] and negatively correlated with tumor T-cell infiltration [7, 13]. However, comprehensive analysis of the immune microenvironment of patients with TRL has not been performed.

In the present study, we compared the immune landscapes of tumors from cervical cancer patients with and without TRL using RNA sequencing. Furthermore, we utilized TCGA data to extend our findings to a larger cohort of TRL patients with cervical and non-cervical cancer with the aim of discovering promising TRL therapeutic targets.

Materials and methods

Patients and sample preparation

Patients with pathologically confirmed squamous cell carcinoma of the uterine cervix without distant metastasis who received definitive chemoradiotherapy or radiotherapy were included in the study. TRL was defined as a white blood cell count exceeding 9000/μL at baseline without any evidence of infection [5]. RNA was extracted from formalin-fixed paraffin-embedded (FFPE) tissue sections with an RNeasy FFPE Kit (Qiagen, Hilden, Germany), and only samples that passed the quality control tests were used for RNA sequencing. RNA quality was assessed using an Agilent 2100 bioanalyzer and an RNA 6000 Nano Chip (Agilent Technologies, Palo Alto, CA), and RNA quantification was performed using an ND-2000 Spectrophotometer (Thermo Fisher Scientific, Waltham, MA). This study was approved by the Institutional Review Board (4-2015-0454), and all patients provided informed consent before inclusion in the study.

RNA sequencing and analysis

Four patients with TRL (TRL^{pos}) and four patients without TRL (TRL^{neg}) were eligible for RNA sequencing. Detailed methods of RNA sequencing are provided in Supplementary materials. Gene counts were normalized by library size, and differential gene expression of genes was analyzed using DESeq2 (version 1.24.0). Differentially expressed genes (DEGs) were determined as those with an adjusted $P < 0.05$ and a $\log_2$ fold change > 1. Gene set enrichment analysis (GSEA) was performed using Broad Institute software (http://software.broadinstitute.org/gsea/index.jsp). Gene ontology (GO) analysis of the gene expression data obtained from MsigDB (http://www.gsea-msigdb.org/gsea/index.jsp) was performed using GSEA and visualized by the Enrichment Map tool in Cytoscape version 3.7.1 (https://cytoscape.org). The enrichment score for gene sets was calculated using a gene set variation analysis (GSVA) with the GSVA R package (version 1.32.0). Heatmaps were generated using the pheatmap package (version 1.0.12).

The cancer genome atlas (TCGA) data acquisition and definition of subgroups

RNA sequencing data and patient clinical information from the TCGA database were obtained for 9984 patients comprising 32 solid tumors using FireBrowse (Broad Institute). A "leukocytosis signature (LS) score" was calculated for each individual using GSVA and was defined as the enrichment score for the gene set derived from the genes differentially expressed between TRL^{pos} and TRL^{neg} tumors. In detail, the GSVA score for significantly down-regulated genes in the TRL^{pos} tumor was subtracted from the GSVA score of significantly up-regulated genes in TRL^{pos} tumor. Patients within the upper quartile of the LS score were defined as LS^{high}, with the remaining patients being defined as LS^{low}.

Immune signature and tumor immune infiltrate analysis

The signature scores for five immune expression signatures, namely the interferon (IFN)-γ response, the transforming growth factor (TGF)-β response, macrophage/monocytes, lymphocyte infiltration, and wound healing, were obtained from a previous paper [14]. These five immune signatures were selected from 160 immune expression signatures that robustly reproduced the co-clustering of the immune signature sets, and signature scores were calculated using GSVA. Data for the fraction of immune cell subsets infiltrating the tissue from the TCGA cohort were calculated

Cancer Immunology, Immunotherapy (2020) 69:1265–1277

1267

Table 1 Patient characteristics of those with TRL ($n=4$) and without TRL ($n=4$)

Patient	Age/sex	Histology	Tumor size (cm)	FIGO stage[a]	TNM stage[b]	Leukocyte count (/μL)	ANC (/μL)	ALC (/μL)	NLR (/μL)	Treatment	Recurrence	PFS (m)	OS (m)	Last f/u status
TRL[pos] 1	37/F	Squamous cell ca., non-keratinizing type	7.0	IIB (IIIB)	T2bN1	15,770	11,380	2650	4.29	CCRT	None	57.8	57.8	Alive
TRL[pos] 2	35/F	Squamous cell ca., keratinizing type	6.8	IVA (IVA)	T4N1	9900	8470	530	15.98	CCRT	Lung metastasis	7.8	58.4	Alive
TRL[pos] 3	66/F	Squamous cell ca., non-keratinizing type	6.6	IVA (IVA)	T4N1	11,850	9450	1660	5.69	RT	Pelvic LN metastasis	3.5	8.3	Dead
TRL[pos] 4	28/F	Squamous cell ca., non-keratinizing type	7.3	IIA (IIIB)	T2a2N1	12,960	8250	2200	3.75	CCRT	Lung metastasis	7.5	16.5	Dead
TRL[neg] 1	76/F	Squamous cell ca., non-keratinizing type	1.9	IIA1 (IIA1)	T2a1N0	6090	4200	1430	2.94	CCRT	None	57.8	57.8	Alive
TRL[neg] 2	56/F	Squamous cell ca., non-keratinizing type	5.0	IB2 (IIIB)	T1b2N1	8010	3710	3340	1.11	CCRT	None	55.7	55.7	Alive
TRL[neg] 3	75/F	Squamous cell ca., non-keratinizing type	5.6	IIB (IIIB)	T2bN1	8370	5300	2400	2.21	CCRT	None	60.8	60.8	Alive
TRL[neg] 4	54/F	Squamous cell ca., non-keratinizing type	3.1	IIB (IIIB)	T2bN0	7320	2970	3890	0.76	CCRT	None	69.4	69.4	Alive

TRL, tumor-related leukocytosis; ANC, absolute neutrophil count; ALC, absolute lymphocyte count; NLR, neutrophil-to-lymphocyte ratio; PFS, progression-free survival; OS, overall survival; CCRT, concurrent chemoradiotherapy; RT, radiotherapy; LN, lymph node

[a]2019 FIGO staging is provided in parenthesis

[b]AJCC 8th edition
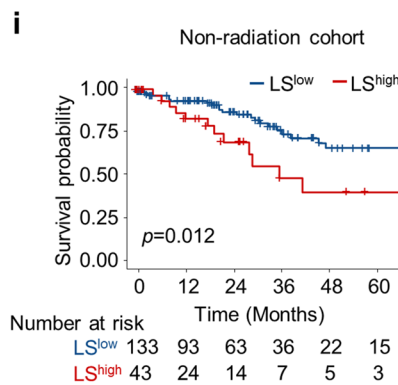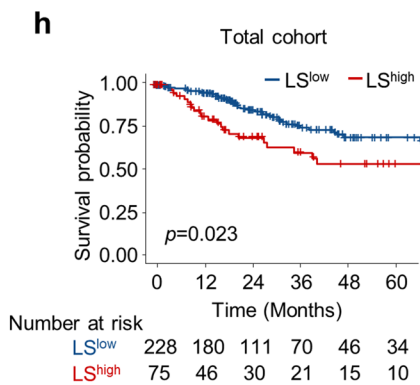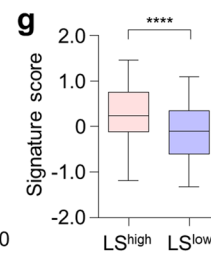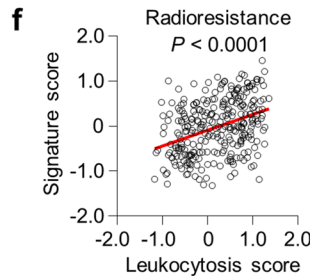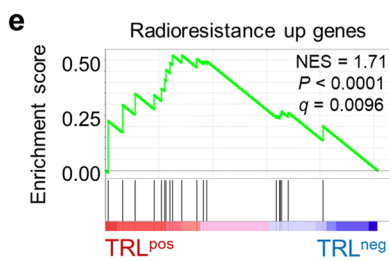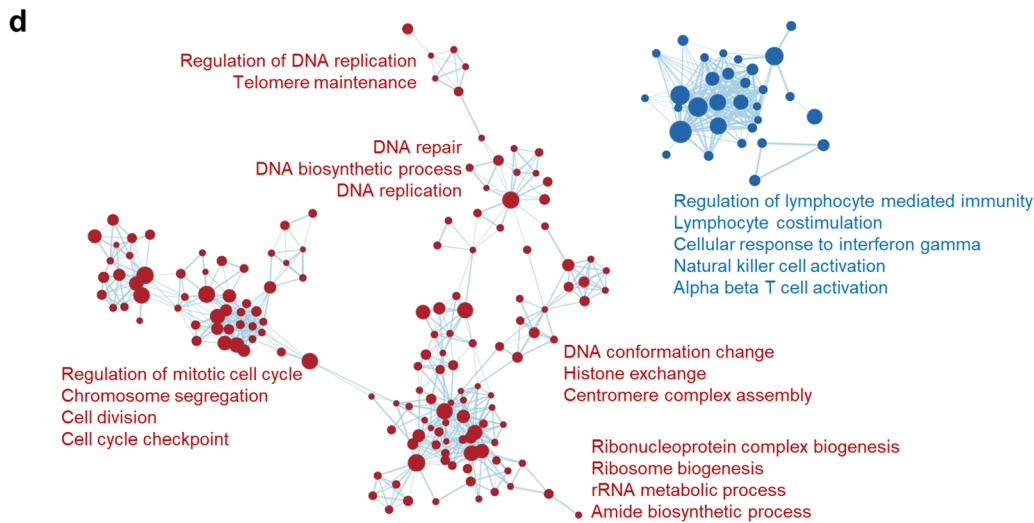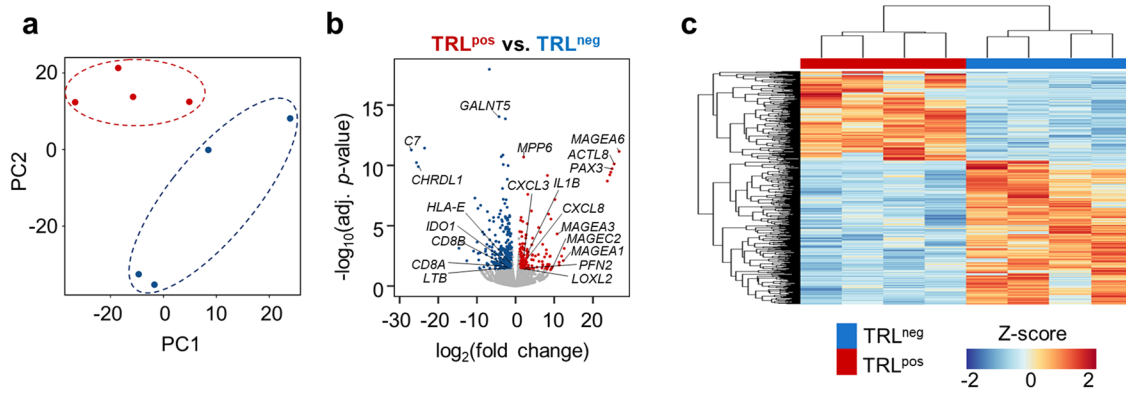
◀**Fig. 1** TRL^pos tumors exhibit a gene expression profile distinct from that of TRL^neg tumors. **a** Principal component analysis of tumors from patients with (TRL^pos; $n=4$) and without (TRL^neg; $n=4$) TRL. **b** Volcano plot demonstrating the differentially expressed genes between the TRL^pos and TRL^neg tumors. The *blue* and *red* dots indicate significantly down- or up-regulated genes in TRL^pos tumors, respectively ($\log_2$fold change > 1, adjusted $P < 0.05$). **c** Unbiased hierarchical clustering analysis of differentially expressed genes in TRL^pos and TRL^neg tumors. **d** Expression levels of gene ontology (GO) gene sets in TRL^pos and TRL^neg tumors. A gene set enrichment analysis (GSEA) was used to identify positive (*red*) and negative (*blue*) enrichment of GO gene sets in TRL^pos tumors. The size of the nodes represents the number of genes in each pathway, and the links represent genes that are shared by two given pathways. Networks were generated using cytoscape. **e** GSEA of the radioresistance gene signature in TRL^pos ($n=4$) and TRL^neg ($n=4$) tumors. **f** Correlation plot between the LS score and radioresistance gene signature score in the TCGA uterine cervical cancer cohort ($n=303$). Signature scores were calculated using a gene set variation analysis (GSVA). **g** Radioresistance gene signature scores in LS^high and LS^low tumors. The lines in the boxplot indicate median values, the boxes indicate the IQR values, and the whiskers extend to 1.5 × the IQR values. **h, i** Overall survival of patients with LS^low tumors and those with LS^high tumors in the whole TCGA cervical cancer cohort (**h**; $n=303$) and patients who did not receive radiotherapy (**i**; $n=176$). Student's t-test (**g**), log-rank test (**h, i**). ****, $P < 0.0001$

using CIBERSORT [15]. The suppressive MDSC gene signature was derived from a previous study that identified the top 100 differentially expressed genes between suppressive MDSCs and monocytes sorted from peripheral blood mononuclear cells [16]. The T cell-inflamed gene expression profile, which is known to predict tumor response to anti-programmed death-1 (PD-1) therapy was calculated by GSVA using a previously reported gene set [17]. The neoantigen load for each patient from the TCGA cohort was obtained from a previous paper [14], which were determined from single-nucleotide variants and indel mutations that were predicted to result in Major histocompatibility complex binding peptides. The T cell receptor (TCR) and B cell receptor (BCR) diversities of patients from the TCGA cohort, which were measured using the Shannon entropy, were obtained from a previous report [14].

Statistical analysis

A Student's *t*-test was performed to compare continuous variables between two groups. Survival curves were generated using Kaplan–Meier curves and compared using a log-rank test. A Cox regression was performed to determine the hazard ratio (HR) for the LS score on survival. A Pearson correlation analysis was performed to determine the correlation between two continuous variables. Two-sided *P*-values < 0.05 were considered significant. All statistical analyses were performed in R version 3.5.1 (http://www.r-project.org) or GraphPad Prism version 6.0 (GraphPad Software Inc., San Diego, CA).

Results

The characteristics of the four TRL^pos patients and the four TRL^neg patients are summarized in Table 1. TRL^pos patients tended to have lower age, larger tumor, and more advanced tumor stage compared to TRL^neg patients. In addition, TRL^pos patients showed predominance of neutrophils among their leukocytes and a higher neutrophil-to-lymphocyte ratio (NLR) compared to TRL^neg patients. All patients had received radiotherapy or chemoradiotherapy. Three of the four TRL^pos patients experienced recurrence, while TRL^neg patients experienced no recurrence. At last follow-up, two patients were alive among the four TRL^pos patients and all TRL^neg patients were alive.

Next, we performed RNA sequencing of tumors obtained from four TRL^pos and four TRL^neg patients. Principal component analysis of TRL^pos and TRL^neg tumor gene expression showed distinct transcriptional landscapes (Fig. 1a). There were 591 differentially expressed genes in TRL^pos tumors ($\log_2$fold change > 1, adjusted $P < 0.05$), of which 227 genes were significantly up-regulated and 364 genes were significantly down-regulated (Fig. 1b; Supplementary Table 1). Unsupervised hierarchical clustering confirmed that the TRL^pos and TRL^neg tumor gene signatures were distinct (Fig. 1c). Genes up-regulated in TRL^pos tumors included those related to cancer–testis antigens (*MAGEA1, MAGEA3, MAGEA6, MAGEC2, ACTL8*), neutrophil chemotaxis (*CXCL3, CXCL8*), inflammatory cytokines (*IL1B*), and epithelial–mesenchymal transition (*LOXL2, PFN2*) [18], whereas down-regulated genes included those related to T cells (*CD8A, CD8B*), T-cell immune response (*HLA-E, IDO1*), and the complement pathway (*C7*) (Fig. 1b, Supplementary Table 1). GSEA using GO gene sets showed that TRL^neg tumors exhibit enrichment in gene sets related to lymphocyte-mediated immunity, cellular response to IFN-γ, and T cell activation (Fig. 1d), while TRL^pos tumors exhibit enrichment in gene sets related to DNA repair, replication, and cell cycle progression, implying the possibility of intrinsic radioresistance in TRL^pos tumors (Fig. 1d). Supporting this, TRL^pos tumors also showed enrichment in radioresistance-related genes (Fig. 1e) [19]. We further assessed the radioresistance signature in the TCGA cohort of uterine cervical cancer patients. Due to the lack of blood count data in the TCGA cohort and as indicative of TRL diagnosis, we calculated the LS score for each tumor, and defined LS^high and LS^low tumors as TRL^pos and TRL^neg tumors, respectively. The radioresistance signature score, derived from the radioresistance-related genes [19] by GSVA, showed a significant correlation with the LS (Fig. 1f), such that LS^high tumors exhibited a significantly higher radioresistance signature score than LS^low tumors (Fig. 1g). Patients with LS^high tumors had significantly lower survival rates than patients
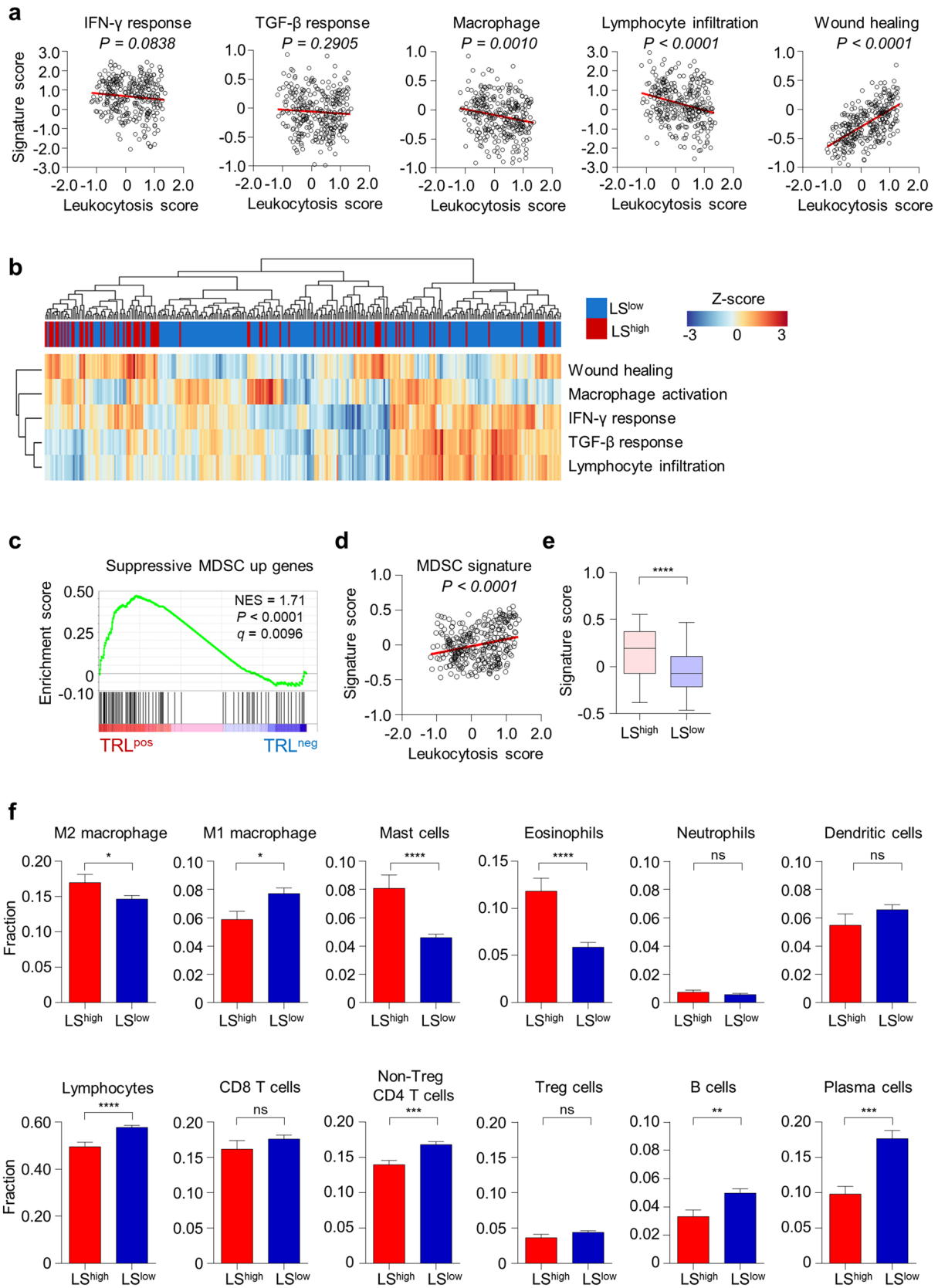
◄**Fig. 2** LS^{high} tumors have a more suppressive immune microenvironment than LS^{low} tumors. **a** Correlation between the LS score and signature scores for the IFN-γ response, the TGF-β response, macrophage, lymphocyte infiltration, and wound healing in the TCGA uterine cervical cancer cohort ($n=303$). **b** Unbiased hierarchical clustering analysis for the signature scores for the IFN-γ response, the TGF-β response, macrophage, lymphocyte infiltration, and wound healing signatures in LS^{high} ($n=75$) and LS^{low} ($n=228$) tumors. **c** GSEA of the immunosuppressive MDSC gene signature in TRL^{pos} ($n=4$) and TRL^{neg} ($n=4$) tumors. **d** Correlation plot between the LS score and the immunosuppressive MDSC gene signature score ($n=303$). **e** Immunosuppressive MDSC gene signature scores in the LS^{high} ($n=75$) and LS^{low} ($n=228$) tumors. The lines in the boxplot indicate median values, the boxes indicate the IQR values, and the whiskers extend to 1.5×the IQR values. **f** The fraction of different immune cell subsets in the LS^{high} ($n=75$) and LS^{low} ($n=228$) tumors. The fractions of cells were derived from CIBERSORT. Bar graphs represent mean and s.e.m. Student's t-test (**e, f**). ns, not significant; *, $P<0.05$; **, $P<0.01$; ***, $P<0.001$; ****, $P<0.0001$

with LS^{low} tumors (Fig. 1h). Although TRL^{pos} or LS^{high} tumors exhibited signatures for radioresistance, a high LS score was still associated with a poor prognosis in patients who did not receive radiotherapy (Fig. 1i), implying that the poor prognosis of patients with TRL may stem not only from the innate radioresistance of tumor cells but also from other factors.

We next investigated the tumor immune microenvironment in uterine cervical cancer patients of the TCGA cohort based on the LS score. The LS score was significantly and negatively correlated with the macrophage/monocyte activation signature and the lymphocyte infiltration signature score and was significantly positively correlated with the wound healing signature score (Fig. 2a). A clustering analysis of LS^{high} and LS^{low} tumors also showed that the LS^{high} tumors were enriched in the cluster with a high wound healing signature score and low macrophage/monocyte activation, IFN-γ response, TGF-β response, and lymphocyte infiltration signature scores (Fig. 2b). However, there were some LS^{high} tumors that exhibited high IFN-γ response, TGF-β response, and lymphocyte infiltration signature scores, implying heterogeneity in the LS^{high} tumors (Fig. 2b). We next evaluated the degree of MDSC activation in the TRL^{pos} and TRL^{neg} tumors. The suppressive MDSC gene signature was significantly enriched in TRL^{pos} tumors (Fig. 2c). In the TCGA cohort, the suppressive MDSC gene signature score was significantly correlated with the LS (Fig. 2d), and LS^{high} tumors exhibited higher suppressive MDSC gene signature scores than LS^{low} tumors (Fig. 2e). The LS^{high} tumors had a higher fraction of M2 macrophages, mast cells, and eosinophils and a lower fraction of M1 macrophages and lymphocytes (Fig. 2f). Among lymphocytes, the fractions of non-Treg CD4 T cells, B cells, and plasma cells were significantly higher in TRL^{neg} tumors (Fig. 2f).

Given the importance of chemotaxis in the recruitment of immune cells to peripheral tissues, we next examined the expression of chemokines. An unsupervised hierarchical clustering of 42 chemokines in 303 uterine cervical tumors demonstrated the clustering of chemokines related to CXCR2, a chemokine receptor that mediates both neutrophil and MDSC trafficking (Fig. 3a). Moreover, the expression of the CXCR2 chemokines *CXCL1*, *CXCL2*, *CXCL3*, *CXCL5*, and *CXCL8* was significantly higher in LS^{high} tumors (Fig. 3b). In addition to chemokines, we also examined the expression of growth factors for neutrophils or monocytes, such as *CSF1* (M-CSF), *CSF2* (GM-CSF), and *CSF3* (G-CSF), and found that LS^{high} tumors had a significantly higher expression of *CSF2* and *CSF3*, but not *CSF1* compared to LS^{low} tumors (Fig. 3c). Thus, LS^{high} tumors showed the potential for enhanced chemotaxis of neutrophils or MDSCs to the tumor site and higher expression of neutrophil- or MDSC-inducing cytokines.

Considering the role of MDSCs in disrupting the effectiveness of immune checkpoint blockade, we next investigated the potential of TRL^{pos} and TRL^{neg} or LS^{high} and LS^{low} tumors to respond to anti-PD-1 therapy. The T cell-inflamed gene signature, which has been shown to predict responses to anti-PD-1 therapy in multiple types of cancer [17], was found to be significantly enriched in TRL^{neg} tumors (Fig. 4a). The T cell-inflamed gene signature score was also higher in LS^{low} tumors, with a borderline significance ($P=0.0581$; Fig. 4b). The neoantigen number, which is also known to be a predictive marker for anti-PD-1 therapy [20], was similar in the LS^{high} and LS^{low} tumors (Fig. 4c). TCR and BCR diversity was significantly lower in the LS^{high} tumors (Fig. 4d).

To extend our findings derived from patients with uterine cervical cancer, we compared the survival of patients with LS^{high} and LS^{low} tumors and the immune signatures of these tumors in the pan-cancer cohort of the TCGA database comprising 32 types of solid tumors and 9984 patients. Patients with LS^{high} tumors exhibited a significantly poorer overall survival compared to those with LS^{low} tumors (HR 1.57, 95% CI 1.48–1.67, $P<0.0001$; Fig. 5a). LS^{high} tumors also had a significantly higher MDSC signature score than LS^{low} tumors (Fig. 5b). As seen in the TCGA uterine cervical cancer cohort, LS^{high} tumors exhibited a higher wound healing signature, but lower IFN-γ response, TGF-β response, macrophage/monocyte activation, and lymphocyte infiltration signatures (Fig. 5c). In terms of chemokine expression, LS^{high} tumors expressed significantly higher levels of *CXCL1*, *CXCL2*, *CXCL3*, *CXCL5*, and *CXCL8* (Supplementary Fig. 1a). In addition, LS^{high} tumors expressed higher levels of *CSF2* and *CSF3* (Supplementary Fig. 1b). We next evaluated the prognostic impact of the LS score in the 32 types of solid tumors. A higher LS score was associated with poorer overall survival not only in uterine cervical cancer but also in adrenocortical carcinoma, bladder urothelial carcinoma, head and neck squamous cell carcinoma, kidney
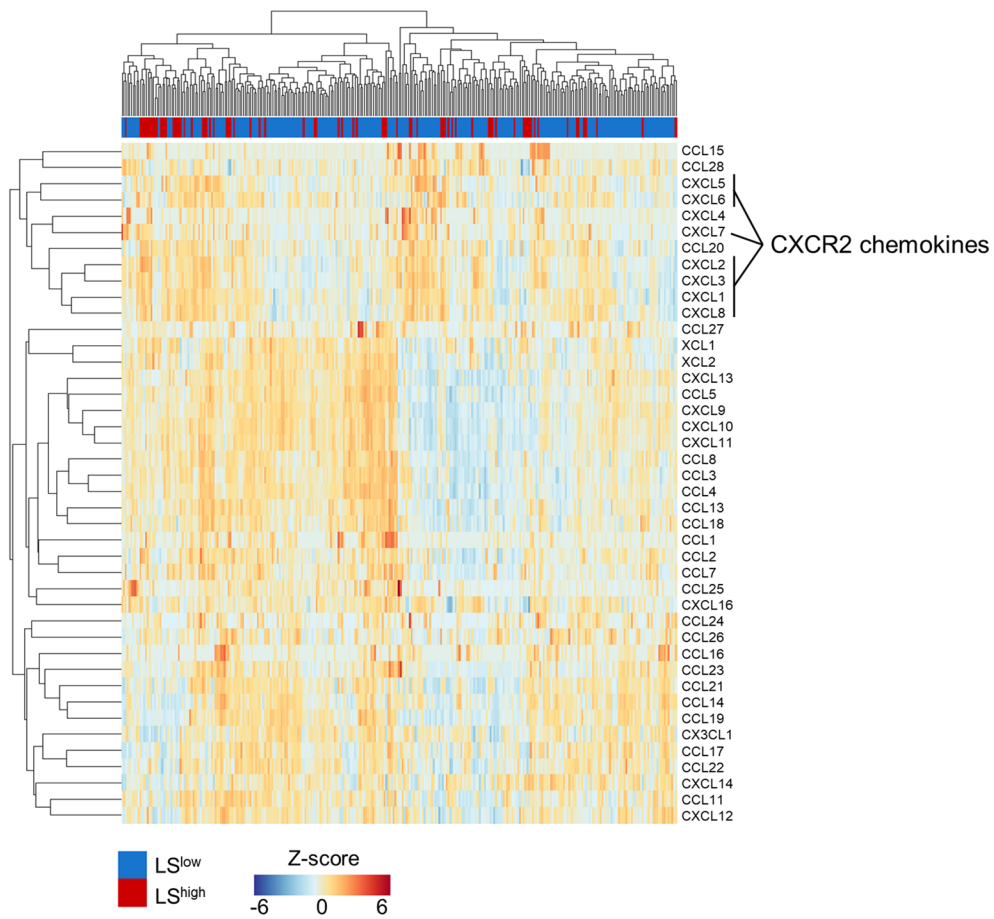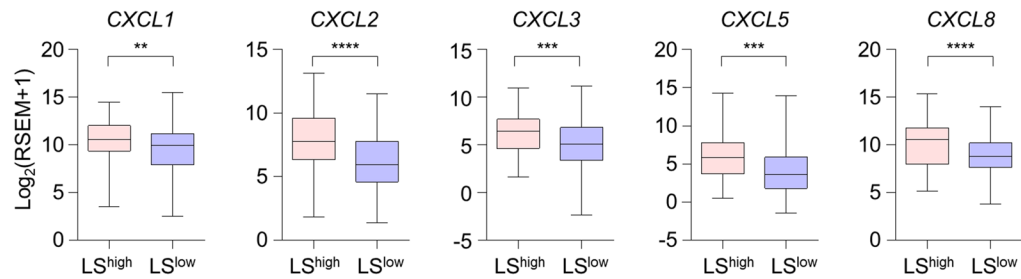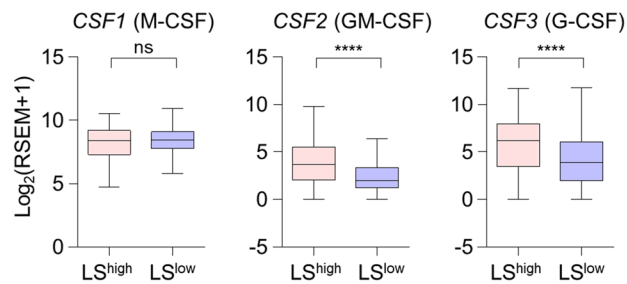
◄**Fig. 3** Chemokine expression in LS^{high} and LS^{low} tumors. **a** Unbiased hierarchical clustering analysis for gene expression of 42 types of chemokine in the LS^{high} ($n=75$) and LS^{low} ($n=228$) tumors in the TCGA uterine cervical cancer cohort. **b** Gene expression of selected CXCR2-related chemokines in LS^{high} ($n=75$) and LS^{low} ($n=228$) tumors. **c** Gene expression of *CSF1*, *CSF2*, and *CSF3* in LS^{high} ($n=75$) and LS^{low} ($n=228$) tumors. The lines in the boxplot indicate median values, the boxes indicate the IQR values, and the whiskers extend to $1.5 \times$ the IQR values. Student's t-test (**b, c**). ns, not significant; **, $P<0.01$; ***, $P<0.001$; ****, $P<0.0001$
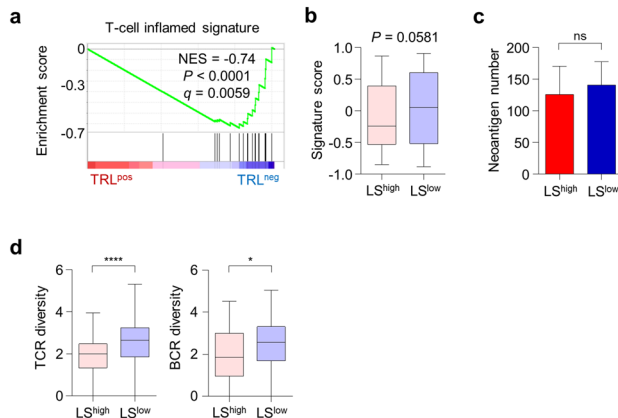
Fig. 4 TRL^{pos} and LS^{high} tumors exhibit features of anti-PD-1 unresponsiveness. **a** GSEA of the T-cell-inflamed gene signature in TRL^{pos} and TRL^{neg} tumors. **b** T-cell-inflamed gene signature scores in LS^{high} ($n=75$) and LS^{low} ($n=228$) tumors. **c** Neoantigen number in LS^{high} ($n=75$) and LS^{low} ($n=228$) tumors. **d** T-cell receptor (TCR) and B-cell receptor (BCR) diversity in LS^{high} ($n=75$) and LS^{low} ($n=228$) tumors. Diversity indicates the Shannon entropy score. The lines in the boxplot indicate the median values, the boxes indicate the IQR values, and the whiskers extend to $1.5 \times$ the IQR values. Bar graphs represent mean and s.e.m. Student's t-test (**b-d**). ns, not significant; *, $P<0.05$; ****, $P<0.0001$

chromophobe, kidney renal clear cell carcinoma, kidney renal papillary cell carcinoma, liver hepatocellular carcinoma, lung adenocarcinoma, mesothelioma, sarcoma, skin cutaneous melanoma, uterine corpus endometrial carcinoma, and uveal melanoma (Fig. 5d).

Discussion

Although a large number of studies have demonstrated the prognostic impact of TRL in various cancer types and treatment settings [4–7], the microenvironment in human TRL^{pos} tumors has not been well studied. Here, we comprehensively characterized the immune microenvironment of TRL^{pos} tumors in patients with cervical cancer, as well as various other types of cancers. TRL^{pos} and TRL^{neg} tumors exhibited distinct transcriptional profiles and TRL^{pos} tumors exhibited increased radioresistant signature, but reduced lymphocyte activation signature. We utilized DEGs from the TRL^{pos}

and TRL^{neg} tumors to derive an LS score and defined LS^{high} and LS^{low} tumors in the TCGA cohort as representative of TRL^{pos} and TRL^{neg} tumors, respectively. Further analysis revealed that LS^{high} tumors exhibit a more suppressive immune microenvironment than LS^{low} tumors, characterized by higher MDSC and wound healing signatures and lower macrophage activation and lymphocyte infiltration signatures. Furthermore, we found that TRL^{pos} or LS^{high} tumors had higher expression levels of CXCR2 chemokines than TRL^{neg} or LS^{low} tumors, suggesting the CXCR2 axis may be a promising target for patients with TRL.

TRL in cervical cancer has been suggested as a distinct clinical entity with a lower response rate to radiation and a higher potential for metastasis or locoregional recurrence [5, 11]. As from the previous report [4], we found that patients with TRL tended to have lower age, larger tumor, and more advanced tumor stage than patients without TRL. Importantly, we found that TRL^{pos} and TRL^{neg} tumors have distinct transcriptional profiles. One of the features of TRL^{pos} tumors was enrichment of radioresistant gene signatures. Extending these findings to the TCGA cohort, we found that patients with LS^{high} tumors also had a higher radioresistant signature and poorer survival than patients with LS^{low} tumors. However, a high LS score was also associated with poorer survival in patients treated without radiation, which implies that the poor prognosis of LS^{high} patients may not be solely attributed to radioresistance. As a result, we focused on examining the immune microenvironment.

TRL^{pos} or LS^{high} tumors exhibited features of suppressive anti-tumor immunity. These tumors were enriched for suppressive MDSC gene signatures, implying that MDSCs are more likely to infiltrate human tumors associated with leukocytosis. In addition, not only MDSCs, but also M2 macrophages, mast cells, and eosinophils were more abundant in LS^{high} tumors. M2-polarized macrophages in tumors, or TAMs [9], mast cells [21], and eosinophils [22] are known to have pro-tumorigenic effects, which supports the suppressive anti-tumor immunity in patients with TRL. TAMs and mast cells are also key players in the chronic wound healing process [23], and we found that LS^{high} tumors exhibit an elevated wound healing process signature. The chronic wound healing process has remarkable similarities with tumor growth since during the wound healing process an immunosuppressive environment is established through the action of a diverse array of immune cells and cytokines [24]. LS^{high} tumors also showed a lower lymphocyte fraction, notably including non-Treg CD4 T cells, B cells, and plasma cells. A higher faction of plasma cells in tumors has been shown to be a predictor of favorable survival, which is associated with tertiary lymphoid structures (TLSs) in the cancer microenvironment [25]. TLSs are ectopic lymphoid organs that develop in non-lymphoid tissues that are composed of a T cell-rich zone and B cell follicle with germinal
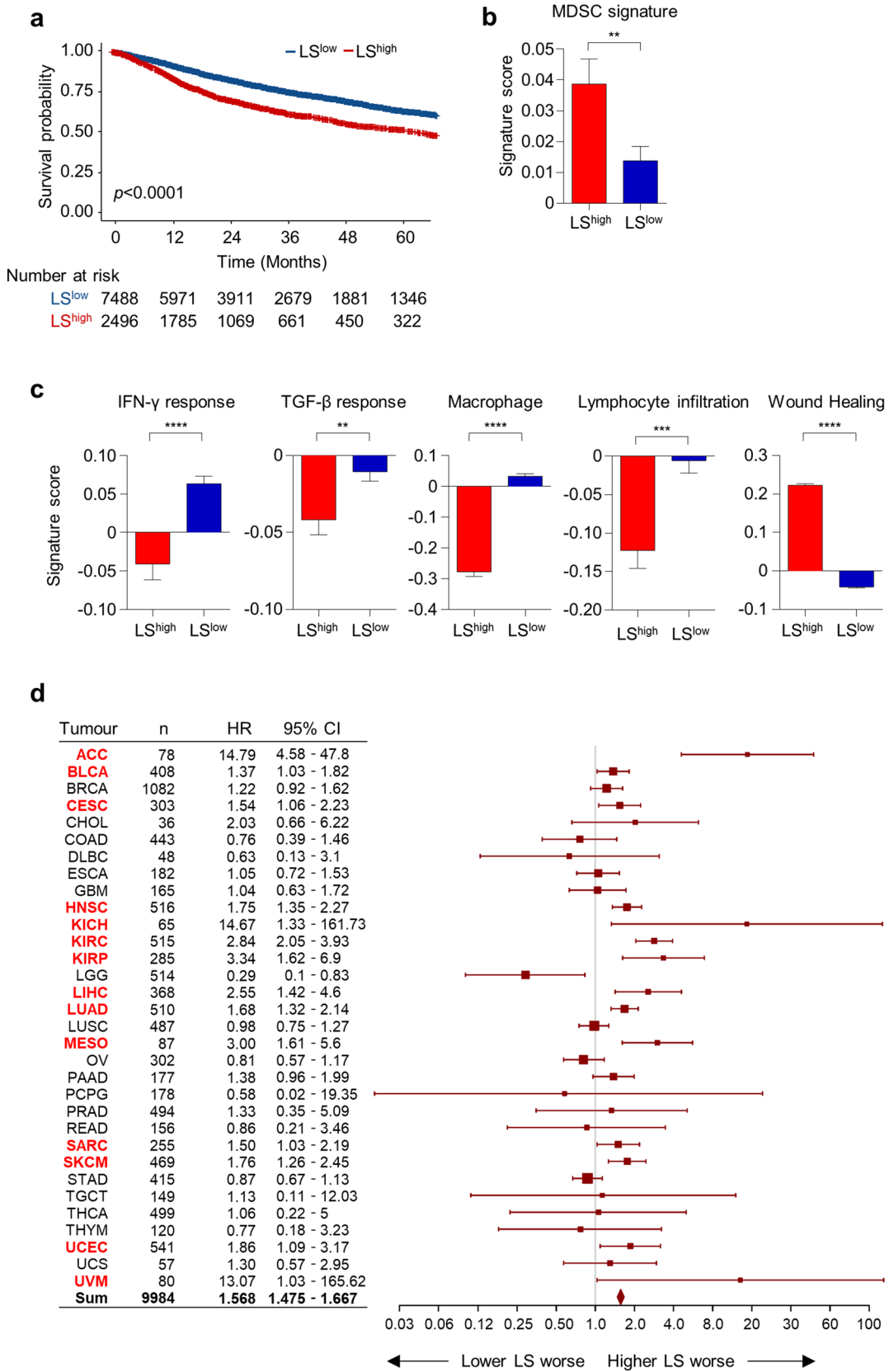
◄**Fig. 5** Pan-cancer analysis of LS^{high} and LS^{low} tumors. **a** Overall survival of patients with LS^{high} and LS^{low} tumors in the TCGA pan-cancer cohort ($n=9984$). **b** Immunosuppressive MDSC gene signature scores in the LS^{high} (n=2496) and LS^{low} (n=7488) tumors. **c** Signature scores for the IFN-γ response, the TGF-β response, macrophage, lymphocyte infiltration, and wound healing signatures in LS^{high} ($n=2496$) and LS^{low} ($n=7488$) tumors. **d** Forest plot demonstrating the hazard ratio and 95% CI of the LS in overall survival among 32 types of solid tumors. Tumor types with a significant association between overall survival and the LS are marked in *red*. Bar graphs represent mean and s.e.m. Student's t-test (**b, c**). Cox regression analysis (**d**). **, $P<0.01$; ***, $P<0.001$; ****, $P<0.0001$

center characteristics, are surrounded by plasma cells, and represent a privileged site for tumor antigen presentation to T and B cells [26]. The presence of TLSs in tumors has been shown to be associated with favorable clinical outcomes [26].

Although the mechanism behind the formation of TRL in humans is yet to be revealed, preclinical studies have suggested that G-CSF secreted from tumor cells may play a role in inducing the generation of MDSCs from the bone marrow [4, 12]. Here, we also found that the expression of *CSF2* (GM-CSF) and *CSF3* (G-CSF) is elevated in LS^{high} tumors. In addition, we also examined the expression of chemokines, since chemotaxis is a crucial process for immune cell recruitment to peripheral tissues. We found that LS^{high} tumors have a higher expression of CXCR2 chemokines, such as *CXCL1*, *CXCL2*, *CXCL3*, *CXCL5*, and *CXCL8* (IL-8). The CXCR2 chemokine axis has been shown to serve a central role in the recruitment of MDSCs leading to tumor progression, and blocking CXCR2 trafficking leads to enhanced anti-tumor effects of anti-PD-1 therapy in mouse tumor models [27, 28]. In humans, IL-8 has been suggested to be a potent chemotactic factor for MDSCs [29]. Therefore, targeting CXCR2 chemotaxis may be an effective strategy to improve the treatment outcome in patients with TRL. In human subjects, an anti-IL-8 antibody showed a favorable safety profile and reduction in serum IL-8 levels; however, there was no objective tumor response in patients with metastatic or unresectable solid tumors [30]. Although blocking the CXCR2 axis itself did not cause dramatic tumor reductions, it may be promising for combination with other treatments, such as radiotherapy, since local radiotherapy has been shown to enhance the production of IL-8 in tumors [31] and increase the frequency of MDSCs [32].

We found that TRL^{high} or LS^{high} tumors exhibit a significantly lower T-cell-inflamed signature which is a well-established gene signature that predicts the response to anti-PD-1 therapy [17]. In addition, LS^{low} tumors exhibited a lower TCR and BCR diversity than LS^{high} tumors. A previous study has also shown that the diversity of peripheral blood T-cell repertoire is negatively correlated with NLR [33]. Furthermore, a higher TCR diversity has been associated with the response to immune checkpoint blockade [34].

Previous studies have also demonstrated that a high absolute neutrophil count or NLR, which is tightly associated with TRL, is associated with a poor response to anti-PD-1 therapy [35–37]. Taken together, tumors associated with leukocytosis are less likely to respond to immune checkpoint blockade and further combinatorial treatments may be needed.

We performed our initial analysis of TRL^{pos} and TRL^{neg} tumors in uterine cervical cancer patients, but found that the findings could be reproduced in multiple types of solid tumors. Cancer types that showed a significant association between a higher LS score and poor overall survival in our study have also been shown to have significant association between TRL or high NLR, with poor prognosis [4–7, 38–40]. However, a higher LS score was significantly associated with poorer survival, but not in all types of cancers. We, thus, suggest that TRL may not have the same prognostic impact in all types of cancers and that the mechanisms for this differential impact in various cancers should be the subject of future investigations.

The current study had some limitations. First, the blood count data lacked in the TCGA cohort, which limited the diagnosis of TRL. As an alternative, we used the DEGs obtained from TRL^{pos} and TRL^{neg} tumors as a surrogate to define TRL in patients in the TCGA cohort. Another limitation is that RNA was extracted from FFPE tissue sections; so as to overcome this limitation, we only used RNA samples that passed quality control tests to assure the accuracy of sequencing data. Moreover, a low number of patients were included for comparison of TRL^{pos} and TRL^{neg} tumors. In addition, TRL^{pos} patients exhibited a heterogeneous clinical response. Although TRL^{pos} patients are suggested to display a distinct clinical entity [4], one of the four patients was recurrence-free for over 4 years, while the others recurred within 1 year post-treatment. Future prospective studies utilizing prospectively collected fresh tissue with blood count data in a larger cohort will better define the immune landscape of tumors associated with leukocytosis.

In conclusion, tumors associated with leukocytosis exhibit a more suppressive immune microenvironment characterized by a higher wound healing signature accompanied by a higher infiltration of MDSCs and TAMs with lower lymphocyte infiltration compared to tumors not associated with leukocytosis. Our findings merit future clinical trials applying novel therapeutics based on the understanding of the distinct immune microenvironment of tumors associated with leukocytosis to improve the treatment outcomes of cancer patients with TRL.

Compliance with ethical standards

References

1. Mantovani A, Allavena P, Sica A, Balkwill F (2008) Cancer-related inflammation. Nature 454(7203):436–444

2. Hanahan D, Weinberg RA (2011) Hallmarks of cancer: the next generation. Cell 144(5):646–674

3. Grivennikov SI, Greten FR, Karin M (2010) Immunity, inflammation, and cancer. Cell 140(6):883–899

4. Mabuchi S, Matsumoto Y, Kawano M, Minami K, Seo Y, Sasano T, Takahashi R, Kuroda H, Hisamatsu T, Kakigano A, Hayashi M, Sawada K, Hamasaki T, Morii E, Kurachi H, Matsuura N, Kimura T (2014) Uterine cervical cancer displaying tumor-related leukocytosis: a distinct clinical entity with radioresistant feature. J Natl Cancer Inst 106(7):dju147

5. Cho Y, Kim KH, Yoon HI, Kim GE, Kim YB (2016) Tumor-related leukocytosis is associated with poor radiation response and clinical outcome in uterine cervical cancer patients. Ann Oncol 27(11):2067–2074

6. Connolly GC, Khorana AA, Kuderer NM, Culakova E, Francis CW, Lyman GH (2010) Leukocytosis, thrombosis and early mortality in cancer patients initiating chemotherapy. Thromb Res 126(2):113–118

7. Martin D, Rodel F, Winkelmann R, Balermpas P, Rodel C, Fokas E (2017) Peripheral Leukocytosis Is Inversely Correlated with Intratumoral CD8 + T-Cell Infiltration and Associated with Worse Outcome after Chemoradiotherapy in Anal Cancer. Front Immunol 8:1225

8. Kumar V, Patel S, Tcyganov E, Gabrilovich DI (2016) The nature of myeloid-derived suppressor cells in the tumor microenvironment. Trends Immunol 37(3):208–220

9. Pathria P, Louis TL, Varner JA (2019) Targeting tumor-associated macrophages in cancer. Trends Immunol 40(4):310–327

10. Ugel S, De Sanctis F, Mandruzzato S, Bronte V (2015) Tumor-induced myeloid deviation: when myeloid-derived suppressor cells meet tumor-associated macrophages. J Clin Invest 125(9):3365–3376

11. Sasano T, Mabuchi S, Kozasa K, Kuroda H, Kawano M, Takahashi R, Komura N, Yokoi E, Matsumoto Y, Hashimoto K, Sawada K, Morii E, Kimura T (2018) The highly metastatic nature of uterine cervical/endometrial cancer displaying tumor-related leukocytosis: clinical and preclinical investigations. Clin Cancer Res 24(16):4018–4029

12. Tavakkoli M, Wilkins CR, Mones JV, Mauro MJ (2019) A novel paradigm between leukocytosis, g-csf secretion, neutrophil-to-lymphocyte ratio, myeloid-derived suppressor cells, and prognosis in non-small cell lung cancer. Front Oncol 9:295

13. Hu X, Li YQ, Li QG, Ma YL, Peng JJ, Cai SJ (2018) Baseline peripheral blood leukocytosis is negatively correlated with T-cell infiltration predicting worse outcome in colorectal cancers. Front Immunol 9:2354

14. Thorsson V, Gibbs DL, Brown SD, Wolf D, Bortone DS, Ou Yang TH, Porta-Pardo E, Gao GF, Plaisier CL, Eddy JA, Ziv E, Culhane AC, Paull EO, Sivakumar IKA, Gentles AJ, Malhotra R, Farshidfar F, Colaprico A, Parker JS, Mose LE, Vo NS, Liu J, Liu Y, Rader J, Dhankani V, Reynolds SM, Bowlby R, Califano A, Cherniack AD, Anastassiou D, Bedognetti D, Rao A, Chen K, Krasnitz A, Hu H, Malta TM, Noushmehr H, Pedamallu CS, Bullman S, Ojesina AI, Lamb A, Zhou W, Shen H, Choueiri TK, Weinstein JN, Guinney J, Saltz J, Holt RA, Rabkin CE, Lazar AJ, Serody JS, Demicco EG, Disis ML, Vincent BG, Shmulevich L (2018) The Immune Landscape of Cancer. Immunity 48(4):812–830 **e14**

15. Newman AM, Liu CL, Green MR, Gentles AJ, Feng W, Xu Y, Hoang CD, Diehn M, Alizadeh AA (2015) Robust enumeration of cell subsets from tissue expression profiles. Nat Methods 12(5):453–457

16. Yaddanapudi K, Rendon BE, Lamont G, Kim EJ, Al Rayyan N, Richie J, Albeituni S, Waigel S, Wise A, Mitchell RA (2016) MIF is necessary for late-stage melanoma patient MDSC immune suppression and differentiation. Cancer Immunol Res 4(2):101–112

17. Ayers M, Lunceford J, Nebozhyn M, Murphy E, Loboda A, Kaufman DR, Albright A, Cheng JD, Kang SP, Shankaran V, Piha-Paul SA, Yearley J, Seiwert TY, Ribas A, McClanahan TK (2017) IFN-gamma-related mRNA profile predicts clinical response to PD-1 blockade. J Clin Invest 127(8):2930–2940

18. Tang YN, Ding WQ, Guo XJ, Yuan XW, Wang DM, Song JG (2015) Epigenetic regulation of Smad2 and Smad3 by profilin-2 promotes lung cancer growth and metastasis. Nat Commun 6:8230

19. Kim HS, Kim SC, Kim SJ, Park CH, Jeung HC, Kim YB, Ahn JB, Chung HC, Rha SY (2012) Identification of a radiosensitivity signature using integrative metaanalysis of published microarray data for NCI-60 cancer cells. BMC Genom 13:348

20. Schumacher TN, Schreiber RD (2015) Neoantigens in cancer immunotherapy. Science 348(6230):69–74

21. Khazaie K, Blatner NR, Khan MW, Gounari F, Gounaris E, Dennis K, Bonertz A, Tsai FN, Strouch MJ, Cheon E, Phillips JD, Beckhove P, Bentrem DJ (2011) The significant role of mast cells in cancer. Cancer Metastasis Rev 30(1):45–60

22. Reichman H, Karo-Atar D, Munitz A (2016) Emerging roles for eosinophils in the tumor microenvironment. Trends Cancer 2(11):664–675

23. Schafer M, Werner S (2008) Cancer as an overhealing wound: an old hypothesis revisited. Nat Rev Mol Cell Biol 9(8):628–638

24. Galdiero MR, Marone G, Mantovani A (2018) Cancer inflammation and cytokines. Cold Spring Harb Perspect Biol 10(8):a028662

25. Kroeger DR, Milne K, Nelson BH (2016) Tumor-infiltrating plasma cells are associated with tertiary lymphoid structures, cytolytic T-cell responses, and superior prognosis in ovarian cancer. Clin Cancer Res 22(12):3005–3015

26. Sautes-Fridman C, Petitprez F, Calderaro J, Fridman WH (2019) Tertiary lymphoid structures in the era of cancer immunotherapy. Nat Rev Cancer 19(6):307–325

27. Steele CW, Karim SA, Leach JDG, Bailey P, Upstill-Goddard R, Rishi L, Foth M, Bryson S, McDaid K, Wilson Z, Eberlein C, Candido JB, Clarke M, Nixon C, Connelly J, Jamieson N, Carter CR, Balkwill F, Chang DK, Evans TRJ, Strathdee D, Biankin AV, Nibbs RJB, Barry ST, Sansom OJ, Morton JP (2016) CXCR2 inhibition profoundly suppresses metastases and augments immunotherapy in pancreatic ductal adenocarcinoma. Cancer Cell 29(6):832–845

28. Highfill SL, Cui Y, Giles AJ, Smith JP, Zhang H, Morse E, Kaplan RN, Mackall CL (2014) Disruption of CXCR2-mediated MDSC

tumor trafficking enhances anti-PD1 efficacy. Sci Transl Med 6(237):237ra67

29. Alfaro C, Teijeira A, Onate C, Perez G, Sanmamed MF, Andueza MP, Alignani D, Labiano S, Azpilikueta A, Rodriguez-Paulete A, Garasa S, Fusco JP, Aznar A, Inoges S, De Pizzol M, Allegretti M, Medina-Echeverz J, Berraondo P, Perez-Gracia JL, Melero I (2016) Tumor-produced interleukin-8 attracts human myeloid-derived suppressor cells and elicits extrusion of neutrophil extracellular traps (NETs). Clin Cancer Res 22(15):3924–3936

30. Bilusic M, Heery CR, Collins JM, Donahue RN, Palena C, Madan RA, Karzai F, Marte JL, Strauss J, Gatti-Mays ME, Schlom J, Gulley JL (2019) Phase I trial of HuMax-IL8 (BMS-986253), an anti-IL-8 monoclonal antibody, in patients with metastatic or unresectable solid tumors. J Immunother Cancer 7(1):240

31. Jin L, Tao H, Karachi A, Long Y, Hou AY, Na M, Dyson KA, Grippin AJ, Deleyrolle LP, Zhang W, Rajon DA, Wang QJ, Yang JC, Kresak JL, Sayour EJ, Rahman M, Bova FJ, Lin Z, Mitchell DA, Huang J (2019) CXCR1- or CXCR2-modified CAR T cells co-opt IL-8 for maximal antitumor efficacy in solid tumors. Nat Commun 10(1):4016

32. Parikh F, Duluc D, Imai N, Clark A, Misiukiewicz K, Bonomi M, Gupta V, Patsias A, Parides M, Demicco EG, Zhang DY, Kim-Schulze S, Kao J, Gnjatic S, Oh S, Posner MR, Sikora AG (2014) Chemoradiotherapy-induced upregulation of PD-1 antagonizes immunity to HPV-related oropharyngeal cancer. Cancer Res 74(24):7205–7216

33. Liu YY, Yang QF, Yang JS, Cao RB, Liang JY, Liu YT, Zeng YL, Chen S, Xia XF, Zhang K, Liu L (2019) Characteristics and prognostic significance of profiling the peripheral blood T-cell receptor repertoire in patients with advanced lung cancer. Int J Cancer 145(5):1423–1431

34. Postow MA, Manuel M, Wong P, Yuan J, Dong Z, Liu C, Perez S, Tanneau I, Noel M, Courtier A, Pasqual N, Wolchok JD (2015) Peripheral T cell receptor diversity is associated with clinical outcomes following ipilimumab treatment in metastatic melanoma. J Immunother Cancer 3:23

35. Tanizaki J, Haratani K, Hayashi H, Chiba Y, Nakamura Y, Yonesaka K, Kudo K, Kaneda H, Hasegawa Y, Tanaka K, Takeda M, Ito A, Nakagawa K (2018) Peripheral blood biomarkers associated with clinical outcome in non-small cell lung cancer patients treated with nivolumab. J Thorac Oncol 13(1):97–105

36. Bagley SJ, Kothari S, Aggarwal C, Bauml JM, Alley EW, Evans TL, Kosteva JA, Ciunci CA, Gabriel PE, Thompson JC, Stonehouse-Lee S, Sherry VE, Gilbert E, Eaby-Sandy B, Mutale F, DiLullo G, Cohen RB, Vachani A, Langer CJ (2017) Pretreatment neutrophil-to-lymphocyte ratio as a marker of outcomes in nivolumab-treated patients with advanced non-small-cell lung cancer. Lung Cancer 106:1–7

37. Ameratunga M, Chenard-Poirier M, Moreno Candilejo I, Pedregal M, Lui A, Dolling D, Aversa C, Ingles Garces A, Ang JE, Banerji U, Kaye S, Gan H, Doger B, Moreno V, de Bono J, Lopez J (2018) Neutrophil-lymphocyte ratio kinetics in patients with advanced solid tumours on phase I trials of PD-1/PD-L1 inhibitors. Eur J Cancer 89:56–63

38. Templeton AJ, McNamara MG, Seruga B, Vera-Badillo FE, Aneja P, Ocana A, Leibowitz-Amit R, Sonpavde G, Knox JJ, Tran B, Tannock IF, Amir E (2014) Prognostic role of neutrophil-to-lymphocyte ratio in solid tumors: a systematic review and meta-analysis. J Natl Cancer Inst 106(6):124

39. Schernberg A, Huguet F, Moureau-Zabotto L, Chargari C, Rivin Del Campo E, Schlienger M, Escande A, Touboul E, Deutsch E (2017) External validation of leukocytosis and neutrophilia as a prognostic marker in anal carcinoma treated with definitive chemoradiation. Radiother Oncol 124(1):110–117

40. Sebastian N, Wu T, Bazan J, Driscoll E, Willers H, Yegya-Raman N, Bond L, Dwivedi A, Mo X, Tan Y, Xu-Welliver M, Haglund K, Jabbour SK, Keane FK, Williams TM (2019) Pre-treatment neutrophil-lymphocyte ratio is associated with overall mortality in localized non-small cell lung cancer treated with stereotactic body radiotherapy. Radiother Oncol 134:151–157